31st Congress of the International Council of the Aeronautical Sciences
Belo Horizonte, Brazil; September 09-14, 2018

FUEL-BURN PENALTIES CAUSED BY IRREGULARITIES IN AIRCRAFT SURFACES (ASTEROID PROJECT)

David Philpott*, Kevin Hackett*, Andrew Shires, Ben Hinchliffe****
***IHS Markit (ESDU), U.K. **University of Leeds, U.K.**

Keywords: *Excrescence, Drag, Transonic*

Abstract

ASTEROID is a research programme part funded by Innovate UK. It provides easy-to-use tools for the estimation of aerodynamic drag and fuel-burn penalties caused by surface irregularities, such as repair patches poorly rigged control surfaces etc. The current status of the estimation procedures, their proposed development and user interfaces are described.

Nomenclature

d	groove depth
D_{basic}	drag of excrescence on flat plate with zero pressure gradient
$\boldsymbol{E}$	position of excrescence (Fig. 3)
h	excrescence height
M	local Mach number
M_∞	free stream Mach number
q	kinetic pressure based on U_e
$\boldsymbol{T}$	position of traverse (Fig. 3)
u	local velocity in boundary layer
u_τ	friction velocity (=
U_e	velocity at edge of boundary layer
$\boldsymbol{V}$	virtual boundary-layer origin without excrescence (Fig. 3)
$\boldsymbol{V'}$	virtual boundary-layer origin with excrescence
x	Distance downstream of excrescence
y	distance from surface
δ	0.995% boundary-layer thickness
$\boldsymbol{\Delta L}$	increment in plate length (Fig. 3)
$\Delta\theta$	Increment in momentum thickness
θ	momentum thickness
ν	kinematic viscosity

1 Introduction

Defect	Fuel penalty per annum	
	Fuel mass	cost*
Inboard slat not fully retracted, increasing the groove at the slat trailing edge from 10 mm to 15 mm.	33,033 kg	$17,010
Spoiler panel number 2 lifted by 3 mm.	8,255 kg	$4,250
Wing lower surface access panel set 1mm above wing surface.	2,064 kg	$1,060
Adjustable aileron rubber seal (3mm leakage gap).	14,447 kg	$7,440
Undercarriage door protrudes 2 mm at inboard edge.	12,384 kg	$6,380
Outboard-flap end seal (3mm leakage gap).	37,150 kg	$19,130

Table 1 Estimated defect fuel costs for medium sized transonic transport aircraft

Table 1 shows costs incurred due to poor rigging of a number of components on an A320 aircraft estimated using current prediction methods [1] with typical annual usage. This information is of value to manufacturers in optimizing tolerance specification and to operators wishing to achieve the best compromise between fuel costs and maintenance costs (including turn-around time penalties). Reference [1] and its associated documents give drag-estimation methods for a large range of excrescences of various sizes. Many of these excrescences can be

* Fuel cost taken as 1.54 $/US gallon

approximately represented by a collection of two-dimensional elements and are small in the sense that they are submerged within the local boundary layer or are of comparable thickness. Typical of such excrescences are repair plates and those given in given in Table 1. Because of the large number of such excrescences on an aircraft, optimum tolerance specification is important.

The ASTEROID* project has two main aims. The first of these is to improve the accuracy and range of applicability of the methods currently used to estimate excrescence drag and the second is to develop interfaces that make it simple for the user to define the characteristics of an excrescence, together with its location on an aircraft, and to calculate the associated drag/financial penalty. This paper outlines the current drag prediction method (and associated deficiencies) for small excrescences. Work, under the ASTEROID project, designed to address these deficiencies is described, together with a brief introduction to new GUI interfaces designed to speed use for both aircraft manufacturers and operators. Particular emphasis is given to typical commercial aircraft operating up to and including transonic cruise speeds.

2 Current Method and Limitations

Drag-prediction methods for small excrescences rely heavily on 2D wind-tunnel data produced using a wall-mounted skin-friction balance over a Mach number range between 0.2 and 2.8, with zero pressure gradient [2]. This gives the basic drag per unit length for a variety of elementary excrescences in a uniform stream.

The edges of 3D excrescences, such as doors and hatches, are built up from 2D elements, such as forward and backwards facing steps, grooves *etc.*, due allowance being made for the alignment of each edge to the local flow external to the boundary layer.

Where the flow external to the boundary layer departs significantly from the idealised uniform stream, *e.g.* on a lifting surface, the effect on the downstream flow is approximated by imposing a step change in boundary-layer momentum thickness at the excrescence location equivalent to the basic drag/unit width of the excrescence, such that:

$$\Delta\theta = 2\frac{D_{basic}}{q}. \qquad (1)$$

A suitable method [3] [4] is then used to determine a magnification-factor by which the basic excrescence drag is multiplied to allow for the effect on the downstream flow. The VGK program, a rapid viscous-coupled full-potential method, can be used for this purpose [4].

This process linearises the problem in the sense that no feedback mechanism is introduced by which changes in the downstream flow can affect the basic drag of the excrescence. Because of this only relatively small disturbances caused by an excrescence can be dealt with.

2.1 Basic drag of excrescence in a subsonic stream

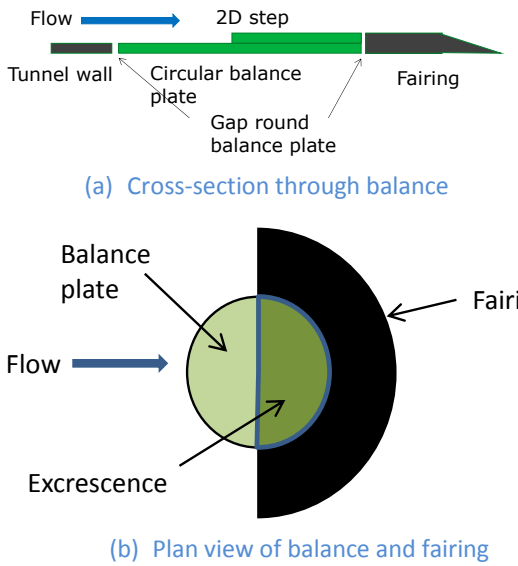

Fig. 1 Measurement of excrescence drag using a skin-friction balance (Reference [2])

Fig. 1 shows an excrescence (in this case a 2D forward-facing step) mounted on the balance plate used in the tests of Reference [2]. The fairing was designed to minimise interference from the downstream flow and to extend the 2D

* The ASTEROID project is part funded by Innovate UK

step mounted on the balance plate to eliminate 3D effects.
Pressure differences in the gap between the balance plate and the tunnel wall were measured and their effect on the balance reading eliminated [2]. The basic drag of the excrescence is determined as the difference between balance readings obtained with the excrescence mounted on the balance plate and the skin-friction drag on the balance plate in the absence of the excrescence.

This measured drag consists of the change in skin friction upstream and downstream of the excrescence on the area covered by the balance plate plus the streamwise force on the vertical surface of the excrescence caused by the local pressure deviation from the freestream value. It is interesting to note that, even in the case of inviscid flow, this latter force would be recorded by the balance because pressure recovery takes place on the tapered aft-edge of the fairing, which is isolated from the balance and therefore not recorded. These problems are considered in [2] and, because only small excrescences heights ($< 0.1\delta$) were tested, are unlikely to be important. For larger excrescence heights covered by the ASTEROID project it is, however, more important to ensure that the effective change in momentum thickness, $\Delta\theta$, is correctly accounted. In a new series of wind-tunnel tests, backed by CFD studies, direct boundary-layer traverses are made upstream and downstream of a number of excrescences, thus allowing a more direct estimate of $\Delta\theta$ to be made.

2.2 Basic drag of excrescence in a supersonic stream and wave drag

A further complication arises if the excrescence is situated in a locally supersonic stream. In this case the value of the basic drag, determined from the balance tests [2], includes a wave-drag component applicable to a test in a uniform supersonic freestream (Fig. 2(a)). However, shock-wave formation (and hence wave drag) differ considerably when the excrescence is located in the small, non-uniform, region of supersonic flow on the upper surface of an aerofoil operating at transonic speed. In this situation the wave strength reduces as distance from the surface increases until it becomes zero at the sonic line bounding the region of supersonic flow (Fig. 2(b).

Much of the wave drag may be generated outside the boundary layer and therefore wave drag is not directly associated with a change in boundary-layer momentum thickness. Thus if wave drag is included in D_{basic} when estimating $\Delta\theta$ from Equation 1, the effect of the excrescence on the downstream flow may be misrepresented and the corresponding magnification factor may be significantly in error. Unfortunately, with the balance tests described in [2], it is not possible to separate wave drag from other forms of drag, making a direct estimate of $\Delta\theta$ difficult.

A more direct estimate of $\Delta\theta$ for the excrescence situated in a uniform stream will be given by the boundary-layer traverse tests that form part of the ASTEROID project.

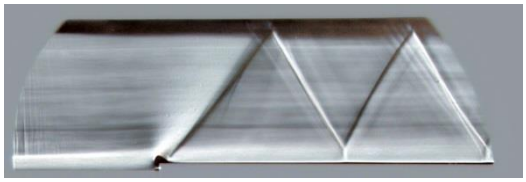

(a) Excrescence in wind tunnel ($M_\infty = 1.4$)

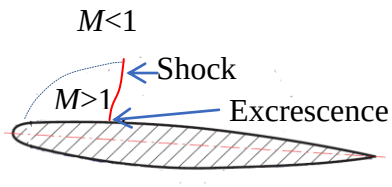

(b) Excrescence on transonic aerofoil

Fig. 2 Excrescence in a supersonic wind tunnel and on the upper surface of a transonic aerofoil

3 Wind-tunnel Test Programme

A series of wind-tunnel tests to extend the range of excrescence geometries covered in [2] and address the problems identified in Section 2 were scheduled at both low and high speed ($M_\infty = 1.4$). In all tests boundary-layer traverses were made at stations upstream and

downstream of the excrescence location using a variety of techniques such as a pitot rake and hot wire (low-speed tests) and LDA (high-speed tests).

4 Calculation of $\Delta\theta$ From Velocity Profiles

Boundary-layer velocity traverses are made upstream and downstream of the excrescence to determine $\Delta\theta$. However, entropy production associated with the basic drag of the excrescence (and hence reflected in $\Delta\theta$) takes place in a complex flow field extending both upstream and downstream of the excrescence. One velocity traverse should therefore be made sufficiently far upstream as to be unaffected by the excrescence. Another traverse should be made sufficiently far downstream to ensure the characteristics typical of a "flat-plate" boundary layer are regained.

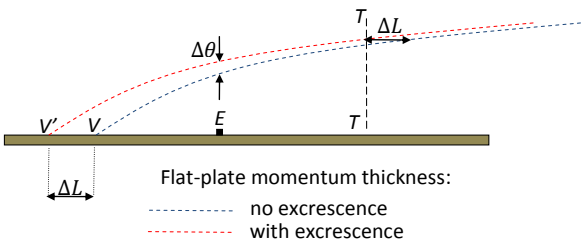

Fig. 3 Determination of $\Delta\theta$ from downstream boundary-layer traverse

Fig. 3 shows how $\Delta\theta$ can be derived from a traverse made at location ***T-T***. Without the excrescence the turbulent boundary layer has the virtual origin ***V*** and the momentum thickness on the flat plate is shown by the blue line. An identical profile, shown by the red line, is constructed starting at the virtual origin ***V'*** so that it passes through the momentum thickness value determined at ***T-T*** in the presence of the excrescence. The required $\Delta\theta$ is the difference between the red and blue lines at the location of the excrescence ***E***. The basic drag of the excrescence is thus equated to the additional drag caused by an extra length of plate, $\boldsymbol{\Delta L}$.

Where compressibility effects are significant, it is important that the appropriate density corrections are included in the calculations [5]. The analysis is further complicated when the wind-tunnel test is conducted at supersonic speed. Because of the of the wave system (Fig. 2(a)), the stream outside the boundary layer is non-homentropic. It may also not be possible to locate a velocity traverse sufficiently far downstream of the excrescence because of the presence of the reflected wave system. This is further discussed in the analysis of the high-speed wind-tunnel test results (Section 6).

5 Low-speed Test Programme and Analysis of Results

The low-speed wind-tunnel test programme covers a range of 2D excrescences. These are shown in Fig. 4 and include forward- and backward-facing steps ((a) and (d)), forward- and backward-facing steps with chamfer ((b) and (e)) and grooves and ridges ((e) and (f)). The range of h/δ for the steps is from 0.009 to 0.909, giving some overlap with the data of [3] at the lower end of the range. For the grooves d/δ is fixed at 0.045 and h/d ranges from 0.0 to 5.0 and l/d from 0.0 to 10.0. h/δ for the ridges varies between 0.02 and 0.25 and l/d between 0.2 and 25.0.

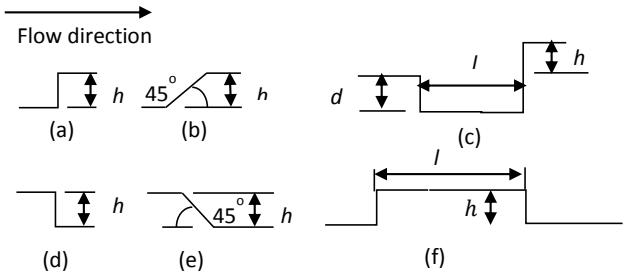

Fig. 4 Excrescence geometries

Two sets of tests were made, one with the excrescences mounted on the floor of a large low-speed tunnel (Cranfield University) and the other on a plate mounted in a smaller low-turbulence tunnel (City University), with artificial transition. In the latter case it was not possible to test backward-facing step configurations. Boundary-layer profiles were measured using a pitot rake in the large low-speed tunnel and a hot-wire traverse in the low-turbulence tunnel. Profiles were measured at a number of stations from $5h$ upstream of the

excrescence to $50h$ downstream. Profiles were measured both with and without the excrescence present. As an example, in this Section and Section 6 special attention is given to the analysis of results for the forward-facing step although similar issues occur with other configurations.

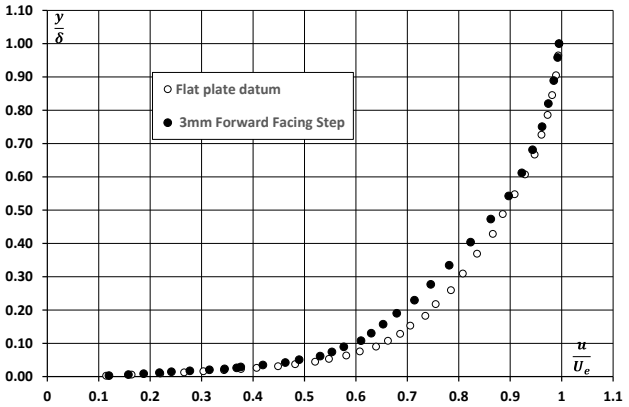

Fig. 5 Effect of excrescence on boundary-layer velocity profile

Fig. 5 shows the effect of a 3mm forward-facing step ($\frac{h}{\delta} = 0.056$) on the boundary-layer velocity profile measured in the low-turbulence tunnel using a hot-wire traverse at a location $25h$ downstream of the excrescence.

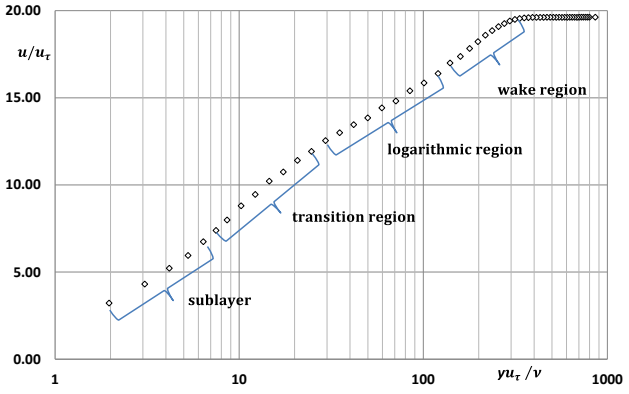

Fig. 6 Boundary-layer regions covered by hot-wire traverse (datum flat-plate flow: low turbulence tunnel with artificial transition)

Fig. 6 shows the measured points in the velocity profile non-dimensionalised using friction velocity and plotted on a logarithmic basis. The classic regions present in a typical turbulent boundary layer are easily identified and measured points are obtained well into the sublayer and sufficiently close to the surface to allow extrapolation to the surface with sufficient accuracy to detect the change in momentum thickness associated with the presence of a small excrescence. Two-dimensionality was confirmed by performing additional traverses on either side of the centre line.

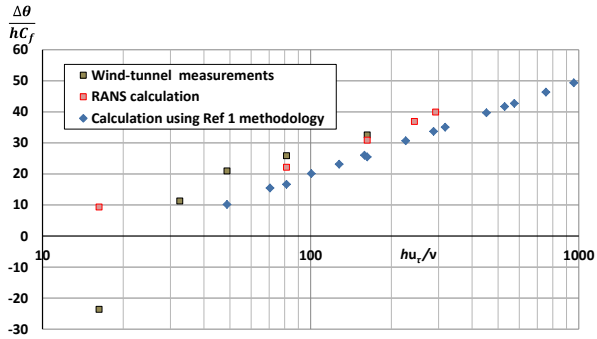

Fig. 7 Variation of $\Delta\theta$ with h (forward-facing step)

Fig. 7 shows the variation of non-dimensionalised $\Delta\theta$ with Reynolds number based on h and u_τ for a forward facing step obtained by subtracting the datum value of θ measured on the flat plate from that obtained in the presence of the excrescence. Values obtained using the current standard method of Reference [1] are also shown, together with RANS calculations made at BHR (Cranfield).

The wind-tunnel results, based on measuring θ, agree well with the RANS calculations and, although they show a similar trend to those derived from [1], are somewhat higher. At the lowest value of h, inaccuracies in measurement and subsequent integration of the velocity profiles to obtain $\Delta\theta$ result in a negative value. To account for the differing values fully, further error analysis will be undertaken both for the current tests and for Reference [2] (see Section 2.1).

Measurements made in the larger wind-tunnel are intended to extend the range of h beyond that covered in [1] and cover configurations, *e.g.* backward-facing steps, that cannot be accommodated in the low-turbulence tunnel. Measurement using the pitot rake is limited so that, typically, no measurements are available in the transition and sublayer regions. Because of this extrapolation of the velocity profile to the surface is required in order to determine the momentum thickness. This was

performed using the method described by Davidson [6], which is applicable to a wide range of boundary-layer velocity profiles. Because of the small difference between the boundary-layer momentum thicknesses with and without the excrescence, values of $\Delta\theta$ produced using this method exhibit a high degree of scatter, although they show the same general trend as Fig. 7. Because of the scatter, the match between results from the two tunnels in the range of overlap is poor, making the use of further wind-tunnel tests to extend the range of excrescence heights dubious until this issue is resolved. An alternative approach is to use CFD to identify trends to allow extrapolation of the low-turbulence tunnel results. The use of CFD will also be investigated as an alternative method to extrapolate velocity profiles where direct measurements are not available close to the surface.

6 High-speed Test Programme ($M_\infty = 1.4$) and Analysis of Results

The cases scheduled covered the geometries shown in Fig. 4, except for configuration (f). Tests were made at a freestream Mach number of 1.4 in a small blowdown supersonic wind-tunnel (Cambridge University) and the boundary-layer velocity profiles measured using a two-component LDA. The excrescence was incorporated into the wind-tunnel floor. For configurations (a), (b), (d) and (e) h/δ values of 0.02, 0.09 and 0.73 were tested. For configuration (c) a single configuration, $d/\delta = 0.05$, $h/d = l/d = 3.7$, was tested.

In the high-speed tests velocity measurement was not possible close to the surface because the flow seeding density was too low to permit adequate an LDA sampling rate. The extrapolation technique described in [6] was therefore also applied to these results. As discussed in Section 2, a further problem is caused by the reflected wave system (Fig. 2(a)), which severely restricts the maximum distance downstream of the excrescence at which a boundary-layer traverse can be made.

Fig. 8 shows a typical velocity profile obtained, using the LDA, on a flat plate at $M_\infty = 1.4$. Fig. 8(b) shows that the measurements cease in the logarithmic region and therefore extrapolation [6] is needed to reconstruct the rest of the profile for the calculation of momentum thickness.

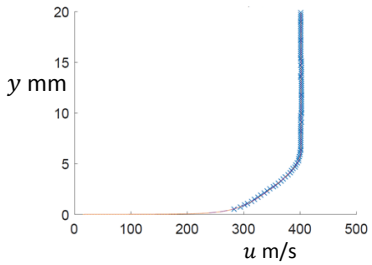

(a) Velocity profile

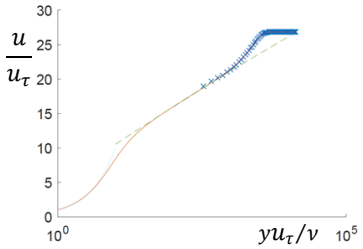

(b) Non-dimensional logarithmic profile

Fig. 8 Flat-plate velocity profile ($M_\infty = 1.4$)

Some judgment is required in constructing the extrapolated curve, using the methods given in Reference [6], because points near the wall which, although sufficiently well seeded to allow recognition by the LDA system, can be inaccurate. A subjective judgement must then be made to exclude them from the extrapolation process.

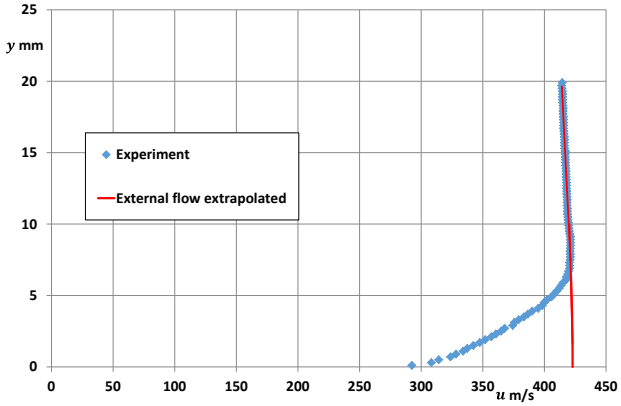

Figure 9 Effect of non-uniform external flow

Figure 9 shows a typical traverse downstream of the excrescence where, because

of the wave system generated in the tunnel and/or the restriction the reflected wave places on the downtream traverse location, the flow external to the boundary-layer is non-uniform. In such cases a hypothetical inviscid flow is extrapolated to the surface to allow the velocity defect in the boundary layer to be determined.

In a similar manner as that suggested for the low-speed tests, a better way to address the uncertainties inherent in the extrapolation processes described above may be to match experimental profiles to a CFD model that can then be used to extrapolate downstream in the absence of reflected waves.

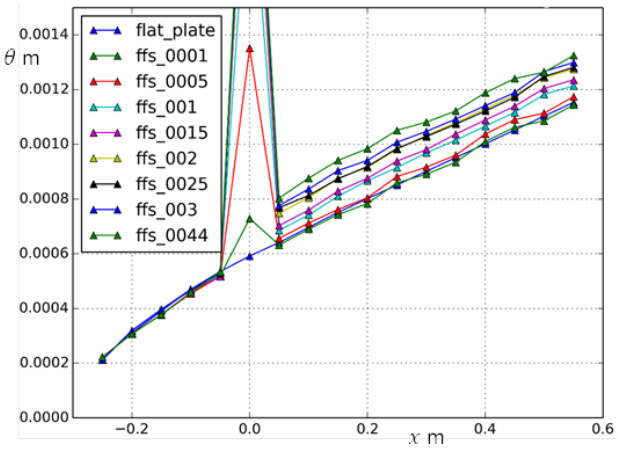

Figure 10 Forward-facing step momentum thickness (CFD calculation, ffs_ denotes step height in m)

Figure 10 shows RANS calculations (using FLUENT with the k-ε turbulence model) for a range of forward-facing step heights. θ was determined at very coarse intervals in x when compared with the computational grid, which accounts for the poor definition in the immediate region of the excrescence.

5.1 Wave drag and magnification factor

Figure 11 shows the variation of $\Delta\theta$ with h derived from CFD calculations (*e.g.* Figure 10) using the method described in Section 2. Values derived from the method of Reference [1], which are based on experiment [2], are also shown. A possible explanation for the large difference (marked as "Wave drag" in Figure 11) is that, in the latter case, the total drag, including the wave drag in the far field, is included in the estimation of $\Delta\theta$. For the reasons given in Section 2.2, both the basic (flat-plate) drag of the excrescence and the magnification factor, applied when the excrescence is mounted on an aerofoil [3], will be in error.

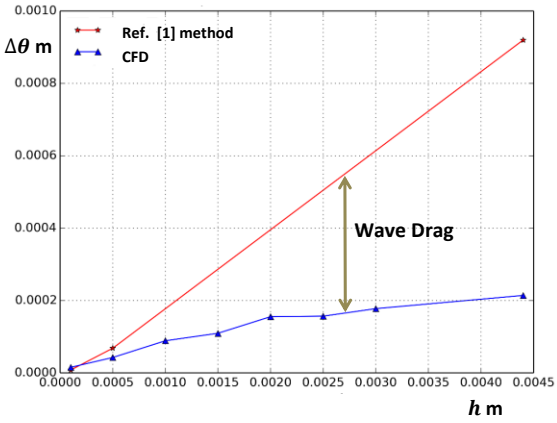

Figure 11 $\Delta\theta$ derived from Ref. [1] and CFD calculation using the method of Section 4

Rather than using balance data measured in a uniform freestream, a preferable procedure may therefore be to determine both the basic drag and magnification factor of an excrescence from $\Delta\theta$ values derived directly from boundary-layer velocity data for the excrescence in a uniform stream. In this case any wave drag occurring within the boundary layer will be accounted. Using VGK with a step change in $\Delta\theta$ at the excrescence location [4] should then provide a better model of the flow in the supersonic patch outside the boundary layer, leading to better determination of the magnification factor.

7 User Interface

A single wing of a transport aircraft may have in the order of 50 components such as control surfaces, inspection panels *etc.* In addition repair patches and retro-fits may be required during the service life of the aircraft. While data are available for some 3D geometries, such as circular and rectangular cavities and protrusions, many, such as those associated with control surfaces, inspection hatches and repair plates, are modeled by an assembly of 2D elements. For example a leading edge slat, in the stowed position is represented by a groove

at its trailing edge together with a smaller groove at each end. To estimate the excrescence drag a separate calculation must be done for each groove which takes into account the local boundary-layer state and the flow external to the boundary layer, including its alignment with the groove. A repair plate may be represented by a polygon of forward and backward facing steps that approximate to its edge. Because of the large number and different types of excrescence on a typical aircraft, a large amount of work is involved in a complete survey to determine excrescence drag.

Because of this, the ASTEROID project has the additional objective of combining currently available methods in a package that makes estimation of the drag of individual excrescences or collections of excrescences on an aircraft easy to perform. The user interface therefore facilitates:

a) easy specification of excrescence geometry, including the specification of complex 3D shapes from 2D elements,
b) easy access to flow conditions at the excrescence location,
c) rapid calculation of the drag of all excrescence types, both 2D and 3D,
d) easy identification of the operational costs associated with the overall excrescence drag and individual excrescences.

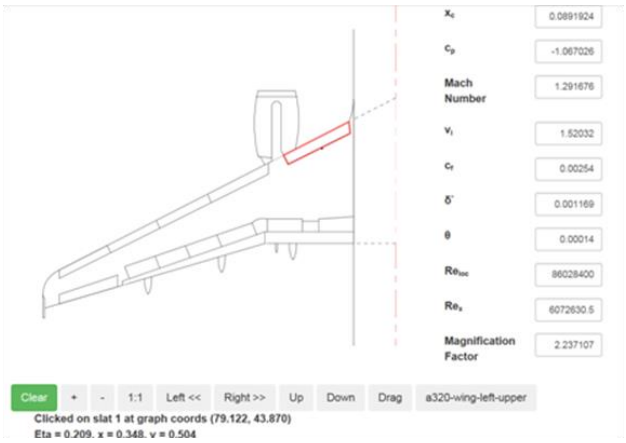

Fig. 12 GUI to select excrescence location and identify local flow parameters

Fig. 12 shows a GUI that addresses requirements (a) and (b). A particular excrescence (in this case the groove at the trailing edge of a leading-edge slat element) is selected using the cursor and local flow conditions at this excrescence are evaluated and presented. Flow-field information incorporated into the program can be generic or, for more accurate calculation, specific to the individual aircraft type. The excrescence type is selected (Fig. 13) and relevant details including dimensions, edge treatment (*e.g.* square, rounded or chamfered) specified. The final calculations ((c) and (d) above) are then performed using routines derived from [1] (and its associated publications) [3] and [4] and user supplied information relating to fuel-burn rates for the aircraft and current fuel costs. When a new excrescence, such a repair plate, is introduced, a GUI is provided to facilitate representation by a series of 2D elements.

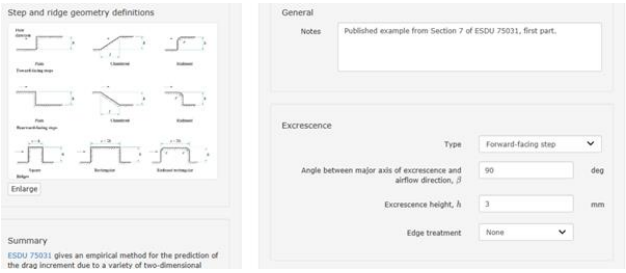

Fig. 13 Excrescence definition

When fully developed, this software package will be adaptable for use in a variety of situations. In the example shown in Fig. 12, for example, it can be used at the design stage to determine the tolerances in the leading edge slat assembly that give the best compromise between manufacturing and operational costs. In service it can be used to determine the economic penalty of retro-fits such as external antennae and to decide on the appropriate design and edge treatment when a repair plate is required.

7 Conclusions

As part of the ASTEROID project, a programme of low- and high-speed wind-tunnel tests was specified to determine $\Delta\theta$ for a series of 2D excrescences by direct boundary-layer measurement. The objective of these tests is to supplement and, where possible, extend the range of the original balance tests [2].

Some difficulty was encountered in achieving satisfactory extrapolation of the boundary layer velocity profiles to the flat-plate surface in the low-speed tests, where measurements were made using a pitot-tube rake and in the high-speed tests in which an LDA was used. Reflected waves in the high-speed tests severely restrict the distance downstream of the excrescence at which a boundary-layer traverse can be made. These problems are exacerbated because $\Delta\theta$ depends on small differences in integrated boundary-layer profiles. Rather than using extrapolation based on [6] better extrapolation may be obtained by CFD calculations matched to local experimental boundary-layer profiles derived from the wind-tunnel tests.

CFD calculation of $\Delta\theta$ for the excrescence in a uniform stream gives considerably higher values than those deduced from wind-tunnel balance measurements of the excrescence drag [1], [2]. This is probably because all wave drag is rcorded by the balance but entropy changes due to the wave system outside the boundary layer will not contribute to $\Delta\theta$.

The wave-drag of the basic excrescence drag in a uniform stream in the wind tunnel will be unrepresentative of the actual wave drag when it is situated in a restricted area of supersonic flow, *e.g.* on the upper surface of a typical transonic transport-aircraft wing. Thus, when the excrescence is in a locally supersonic flow patch, some modification to the current drag accounting procedures, including the magnification factor used to account the effect of the external flow field, may be required.

A GUI-based software package to facilitate the calculation of excrescence drag for both design and operation is described.

8 References

[1] ESDU, An Introduction to aircraft excrescence drag, *ESDU 90024 (with amendments A to C)*, IHS Markit (ESDU), 2016.

[2] Gaudet L and Winter K. Measurement of the drag of some characteristic aircraft excrescences immersed in turbulent boundary layers. *AGARD Conference Proceedings No. 124 on Aerodynamic Drag*, Izmir, Turkey, Paper 4-1, 1973.

[3] ESDU, Simplified method for the prediction of aerofoil excrescence drag magnification factor for turbulent boundary layers at subcritical Mach numbers, *ESDU 91028*, ESDU, 1991.

[4] ESDU, VGK method for two-dimensional aerofoil sections, Part 4, estimation of excrescence drag at subsonic speeds, *ESDU 98031*, IHS (ESDU), 1998.

[5] Green J, Weeks D and Brooman J, Prediction of turbulent boundary layers and wakes in compressible flow by a lag-entrainment method, *Aeronautical Research Council R&M No. 3791*, ARC, 1977.

[6] Davidson T, Effect of incoming boundary layer state on flow development downsteam of a normal shock wave-boundary layer interaction, *PhD Thesis*, Cambridge University, 2016.

9 Contact Author Email Address

mailto: david.philpott@ihsmarkit.com

Copyright Statement